Journal of Molecular Structure 1298 (2024) 137052

Contents lists available at ScienceDirect

Journal of Molecular Structure

journal homepage: www.elsevier.com/locate/molstr

Synthesis, crystal structure and screening for anticonvulsant and antianxiety activities of three new Ni(II), Cu(II), and Zn(II) dithiocarbamate complexes

Anupam Singh [a], Rajesh Kumar [b], Kunal Shiv [a], Shivendra Kumar Pandey [a], M.K. Bharty [a], R.J. Butcher [c], Lal Bahadur Prasad [a,*]

[a] Department of Chemistry, Institute of Science, Banaras Hindu University, Varanasi 221005, India
[b] Department of Pharmacology, Maharaja Agrasen School of Pharmacy, Maharaja Agrasen University, Solan, Himachal Pradesh, 174103, India
[c] Department of Chemistry, Howard University, 525 College Street NW, Washington DC 20059, USA

ARTICLE INFO

Keywords:
Dithiocarbamate
Complex
Crystal structures
Thermogravimetric analysis (TGA)
Anticonvulsant activity
Antianxiety activity

ABSTRACT

A potassium N-(4-fluorobenzyl) N-(naphthalen-1-ylmethyl) dithiocarbamate ligand (fbnm) has been isolated in a basic medium and its Ni(II), Cu(II), and Zn(II) complexes **1**–**3** were synthesized. All new compounds have been characterized by elemental analyses, magnetic susceptibility, IR, NMR, and UV–Vis techniques. Complexes **2** and **3** have been further characterized by single-crystal X-ray diffraction data. Zn(II) complex adopts tetrahedral geometry whereas Ni(II) and Cu(II) complexes adopt square planar geometry around the metal ions. In addition, the bite angles found around the metal chelate rings in complexes **2** and **3** suggest that these geometries are slightly distorted from regular geometry. Complexes **2** and **3** are stabilized by intermolecular C—H···S, C—H···π and CH···F interactions. The thermal degradations of metal complexes **1**–**3** have been examined by TG-DTA data which designates that metal sulfide is formed as the final entity. The anticonvulsant activity of ligand fbnm and its Ni(II), Cu(II), and Zn(II) complexes have been tested through MES test and PTZ induced convulsion test and found that complex **2** may be used as an anticonvulsant compound in the future by further biochemical or neurotransmitter estimations to control the onset of generalized tonic-clonic seizures. The antianxiety activity has also been performed *via* Elevated plus maze and Open field test and observed that all synthesized compounds are non-significant for anti-anxiety effect.

1. Introduction

Epilepsy is a common condition characterized by repeated, persistent seizures that are typically brought on by excessively short electrical discharges in a cluster of brain cells [1]. In epilepsy, the regular pattern of brain activity is disrupted, resulting in bizarre feelings, thoughts, behaviors, convulsions, muscle spasms, and loss of consciousness can also occasionally occur [2]. Nearly 80 % of epilepsy patients, according to the World Health Organization (WHO), reside in developing nations and receive insufficient medical care [3]. Numerous antiepileptic medications are available to treat different types of seizures with the goal of reducing seizure frequency and intensity while posing a manageable risk of adverse effects for instance, phenytoin, carbamazepine, ethosuximide and sodium valproate are used to inhibit seizures [4,5]. Most antiepileptic medications are not effective at controlling seizures in all patients, and they frequently have unpleasant side effects like depression, neurotoxicity, sedation, ataxia, and hypnosis [5,6]. There is a considerable desire for novel anticonvulsants since the unfavorable side effects of the presently used medications frequently make therapy challenging. Therefore, it is crucial and difficult for researchers in medicinal chemistry to work on developing safer and more effective antiepileptic medications.

The current era has witnessed there is a noticeable increase in the design of metal complexes as medications and diagnostic tools [7]. Numerous metal complexes, such as metal-mediated antibiotics, antibacterial, antiviral, antiparasitic, radio sensitizing agents, and anticancer chemicals, are already in clinical use and inspire continuing research for new metallodrugs [8,9]. A few reports are also available on the use of the metal complexes as effective anti-convulsant drugs for instance, Veitia et al. has reported anticonvulsant property of copper(II)

* Corresponding author.
E-mail address: lbprasad@bhu.ac.in (L.B. Prasad).

https://doi.org/10.1016/j.molstruc.2023.137052
Received 3 October 2023; Received in revised form 31 October 2023; Accepted 9 November 2023
Available online 11 November 2023
0022-2860/© 2023 Elsevier B.V. All rights reserved.

complex containing antiepileptic drug sodium salt of valproic acid and 1,10-phenanthroline (*o*-phen) [10]. Shanmugakala et al. has shown Co, Ni and Cu complexes of 2,4-bis(indolin-3-one-2-ylimino)−6-phenyl-1,3,5-triazine and evaluated them for anticonvulsant activity [11]. Subudhi et al. has reported Schiff base derived ligand based on Isatin and glycine and its Co (II), Cu (II) and Zn (II) complexes and investigated their anticonvulsant action [12]. Kurdekar et al. has also investigated the anticonvulsant properties of 4-aminoantipyrine-based Schiff-base metal complexes [13]. The naproxen-based metal complexes were also reported by Hasan et al. for in *vivo* antinociceptive, anxiolytic, CNS depressant, and hypoglycemic activities [14]. Kulkarni et al. has reported a novel Cu(II) and Zn(II) complexes of triazolo-quinoline derivatives and investigated for acute toxicity and in vitro anticonvulsant activity in Wistar rats [15].

Dithiocarbamate or carbamodithioate (CDT) ligands are eminent coordinating agents for metals and they are important in medicine as well [16,17]. For instance, the clinical usage of the diethyldithiocarbamate anion, Et_2CNS_2, as a remedy for copper poisoning, often known as Wilson's illness [18]. They are proven to have wide spectrums of biological activities including insecticidal, antifungal, antibacterial and anticancer activity [19–21]. Additionally, some of its derivatives can strongly block the replication of human rhinoviruses, cause coxsackievirus myocarditis, and cause T-cells to undergo apoptosis [22]. The function of various important proteins involved in apoptosis, oxidative stress, transcription, proteosome function, and as antioxidants and immunosuppressive agents has also been altered by the CDT's [23,24]. Complexes of the CDT exhibit higher antibacterial and antifungal activity than free ligand [25]. Several reports are available of synthesis and characterization of symmetrical as well as unsymmetrical CDT derived ligands and their metal complexes (Ni, Cu, Zn, Pt, Pd, Sn, Co, Cd etc.) [26–28]. Nickel complexes of CDT derived ligands are reported as useful precursor of synthesis of NiS nanoparticles and pre-catalyst in water oxidation [29,30]. Cu and Zn complexes containing CDT derived ligands are investigated for their antibacterial, antifungal, anticancer activities and as dye sensitizer in DSSC [31–33]. Based on the literature carbamoditioate based ligands and its metal complexes are not explored for their anticonvulsant and anti-anxiety activity.

Keeping in mind herein we reports the synthesis spectroscopic and structural characterization of carbamodithioate based ligand (4-fluorobenzyl)(naphthalen-1-ylmethyl)carbamodithioate and its metal complexes (M= Ni(II), Cu(II), Zn(II)). The anticonvulsant and antianxiety activity of CDT and its complexes has been investigated for the first time and found them efficient agent.

2. Experimental

2.1. Chemicals

All the experiments under this research work were performed in open environment at required temperature and normal pressure. All the solvents and chemicals were commercially available synthesis-grade materials (Merck/Sigma-Aldrich/SD Fine/Avra/TCI) and used as received without further purification.

2.2. Analytical characterizations

IR spectra of all synthesized compounds were recorded on a Perkin Elmer FTIR spectrometer in the range 4000 cm^{-1} to 400 cm^{-1} by making their pellets with KBr [34]. The melting point of all the compounds were checked in an open capillary with the help of EZ-Melt automated melting point apparatus. Elemental analysis for C, H, and N was performed by CHN analyzer (Model-CE-440 Elemental Analyzer Exeter Analytical, Inc). The metal complexes were analysed for their metal content after destroying the organic ligand first with aqua regia and then with conc. H_2SO_4. Nickel, copper, and zinc were estimated gravimetrically as Ni(dimethylglyoximate)$_2$, Cu(salicylaldoximate)$_2$, and $ZnNH_4PO_4$, respectively, following the procedure recommended by Vogel. UV–vis spectra of ligand and its metal complexes were recorded by making their 10^{-5} M solution in dichloromethane (DCM) and chloroform (50:50) using a spectrometer {Model- Cary (60 UV–Vis)} from Agilent, USA made. High resolution mass spectrum of each compound was obtained from instrument SCIEX Model- X500R QTOF and data were produced as *m/z* values. ^1H and ^{13}C NMR spectra of the ligand and its diamagnetic complexes were recorded on a JEOL ECZ 500 MHz FT NMR spectrometer and Bruker AVANCE NEO 600 MHz NMR spectrometer (@ SATHI BHU) in DMSO-d_6 and chloroform-d solvent using tetramethyl silane (TMS) as an internal reference. Chemical shift (δ) values are given in parts per million (ppm) downfield from TMS and coupling constant (J) values are quoted in hertz (Hz). Thermal decomposition study of the metal complexes was performed in temperature ranges 30–700 °C in nitrogen atmosphere with elevated temperature rate 10 °C per minute using STA 6000TG/DTA Thermogravimetric Analyzer procured from Perkin Elmer. The single crystal X-ray diffraction data of complexes were recorded using X-ray Diffraction (Sc.) System (Make: Rigaku; Model: Xtalab Synergy i) at Central Discovery Centre (CDC), BHU.

2.3. Synthesis of the ligand

Synthesis of potassium N-(4-fluorobenzyl) N-(naphthalen-1-ylmethyl) dithiocarbamate ligand (fbnm): Potassium salt of the ligand (fbnm) and its Ni(II), Cu(II), and Zn(II) complexes were prepared by adopting Scheme 1. For preparing the ligand (fbnm), 10 mmol (1.358 ml) α-naphthaldehyde and 10 mmol (1.143 ml) 4-fluorobenzylamine were taken into 25 ml of ethanol and refluxed them for 12 h at 90 °C to get corresponding Schiff base which was further reduced into secondary amine by $NaBH_4$ at 0 °C using methanol as solvent. The secondary amine was extracted by separating funnel using DCM and water as solvents and then DCM solvent was removed from secondary amine using rotary evaporator. Further secondary amine was dissolved into tetrahydrofuran (THF) and solution was cooled upto ice cold condition and then KOH (10 mmol) and CS_2 (10 mmol) were added and stirred for 10 h to get the potassium salt of desired ligand which was further dried using rotary evaporator. The obtained product was kept into refrigerator in diethyl ether for 2 days and filtered to get yellow solid product which was dried over silica [35]. Yield: 3.1882 g, 84 %; Melting point: 295 °C (uncorrected); Anal. Calcd. For $C_{19}H_{15}NS_2FK$: C 60.13; H 3.98; N 3.69, Found: C 59.44; H 4.21; N 3.57. IR (KBr, cm^{-1}): 1004 ν(C-S), 1212 ν(C—N), 1505 ν(C═N). UV–Vis (DCM:$CHCl_3$ 50:50, nm) λ_{max} =286. ^1H NMR (500 MHz, DMSO-d_6, δ, ppm): 8.07–7.01 (m, 11H, aromatic protons), 5.75 (s, 2H, methylene protons of -C$\underline{H}_2$C$_{10}$H$_7$), 5.33 (s, 2H, methylene protons of -C$\underline{H}_2$C$_6$H$_4$F). ^{13}C {^1H} NMR (125 MHz, DMSO-d_6, δ, ppm): 217.15 (-CS_2), 162.46, 160.53, 135.39, 134.47, 133.86, 131.81, 129.80, 129.73, 128.89, 127.48, 126.45, 125.93, 125.40, 124.38, 115.19, 115.03 (aromatic carbons), 53.31 (methylene carbon of -C$\underline{H}_2$C$_{10}$H$_7$), 52.59 (methylene carbon of -C$\underline{H}_2$C$_6$H$_4$F). HRMS ($C_{19}H_{15}NS_2FK$): calcd. *m/z* for $[M]^+$= 379.0267, found *m/z* for $[M]^+$= 379.0342.

2.4. Synthesis of metal complexes

Potassium salt of ligand (fbnm) (1 mmol, 0.3795 g) was dissolved in methanol and then methanolic solution of corresponding metal (Ni, Cu, and Zn) acetate (0.5 mmol) was added dropwise to it and stirred for 2 h. A green/brown/white precipitates were obtained for Ni, Cu and Zn complexes, respectively, which were filtered, washed, and dried over silica. Crystals of Cu and Zn complexes were grown through slow evaporation of their methanolic solution.

[Ni(fbnm)$_2$] (1): Yield 0.577 g, 78 %; Melting point: 276 °C (uncorrected). Anal. Calcd. For $C_{38}H_{30}N_2S_4F_2Ni$: C 61.71, H 4.09, N 3.79, Ni 7.94; Found: C 60.08, H 3.83, N 3.58, Ni 7.50. IR (KBr, cm^{-1}): 1015 ν(C-S), 1222 ν(C—N), 1505 ν(C═N), 490 ν(Ni-S). UV–Vis (DCM:$CHCl_3$

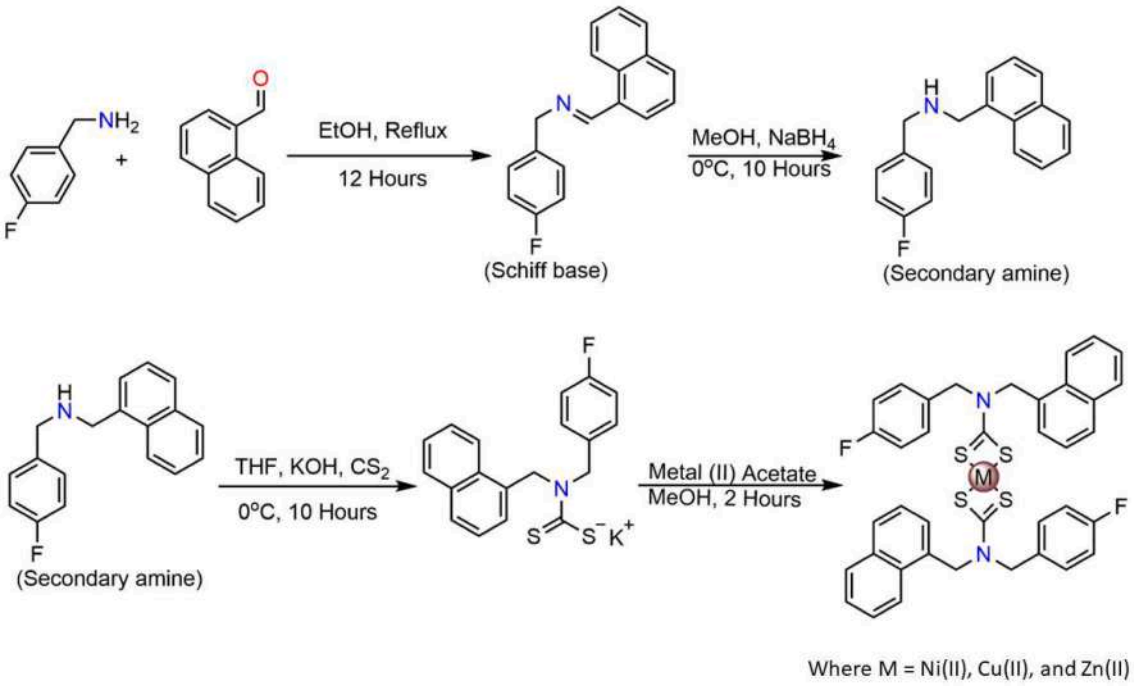

Scheme 1. Schematic representation of synthesis of ligand and metal dithiocarbamate complexes.

50:50, nm) λ_{max} =275 nm,330 nm, 400 nm. ^{1}H NMR (600 MHz, DMSO-d_6, δ, ppm): 7.95–7.09 (m, 22H, aromatic protons), 5.26 (s, 4H, methylene protons of -$CH_2C_{10}H_7$), 4.75 (s, 4H, methylene protons of -$CH_2C_6H_4F$). ^{13}C {^{1}H} NMR (125 MHz, DMSO-d_6 and chloroform-*d*, δ, ppm): 207.72 (-CS_2), 162.49,160.86,133.35,130.59,130.27,130.01, 129.96,128.98,128.74,128.69,126.77,126.19,125.42,122.77,115.45, 115.31 (aromatic carbons), 51.08 (methylene carbon of - $CH_2C_{10}H_7$), 50.01 (methylene carbon of -$CH_2C_6H_4F$). HRMS ($C_{38}H_{30}N_2S_4F_2Ni$): calcd. *m/z* for $[M+H]^+$= 739.0687, found *m/z* for $[M+H]^+$= 739.0690.

[Cu(fbnm)$_2$] (2): Yield: 0.632 g, 85 %; Melting point: 251 °C (uncorrected). Anal. Calcd. For $C_{38}H_{30}N_2S_4F_2Cu$: C 61.31, H 4.06, N 3.76, Cu 8.54; Found: C 60.28, H 3.76, N 3.51, Cu 8.73. IR (KBr, cm^{-1}): 1015 ν(C-S), 1222 ν(C—N), 1508 ν(C═N), 490 ν(Cu-S). UV–Vis (DCM:$CHCl_3$ 50:50, nm) λ_{max} =276 nm, 440 nm. HRMS ($C_{38}H_{30}N_2S_4F_2Cu$): calcd. *m/z* for $[M+H]^+$= 744.0629, found *m/z* for $[M+H]^+$= 744.0621.

[Zn(fbnm)$_2$] (3): Yield: 0.612 g, 82 %; Melting point: 206 °C (uncorrected). Anal. Calcd. For $C_{38}H_{30}N_2S_4F_2Zn$: C 61.16, H 4.05, N 3.75, Zn 8.76; Found: C 60.35, H 3.70, N 3.53, Zn 8.44. IR (KBr, cm^{-1}): 1019 ν(C-S), 1224 ν(C—N), 1508 ν(C═N), 489 ν(Cu-S). UV–Vis (DCM:$CHCl_3$ 50:50, nm) λ_{max} =272 nm. ^{1}H NMR (500 MHz, DMSO-d_6, δ, ppm): 7.98–7.09 (m, 22H, aromatic protons), 5.53 (s, 4H, methylene protons of -$C\underline{H}_2C_{10}H_7$), 5.07 (s, 4H, methylene protons of -$C\underline{H}_2C_6H_4F$). ^{13}C {^{1}H} NMR (125 MHz, DMSO-d_6, δ, ppm): 208.10 (-CS_2), 163.02, 161.08, 133.92, 132.38, 131.23, 130.14, 130.08, 129.20, 128.57, 127.06, 126.57, 126.01, 124.90, 123.60, 115.87, 115.70 (aromatic carbons), 56.59 (methylene carbon of - $C\underline{H}_2C_{10}H_7$), 55.67 (methylene carbon of -$C\underline{H}_2C_6H_4F$). HRMS ($C_{38}H_{30}N_2S_4F_2Cu$): calcd. *m/z* for $[M+H]^+$= 745.0625, found *m/z* for $[M+H]^+$= 745.0597.

2.5. Animals

Male Charles Foster rats weighing 200–280 g were provided by the Central Animal House, Institute of Medical Sciences, Banaras Hindu University. The rats were kept in the animal facility of the Department of Pharmacology, IMS-BHU, with standard food and water supply. The temperature in the animal house was maintained at a constant of 25°C±2°C. The research proposal was approved by the Central Animal Ethical Committee of Banaras Hindu University (Reg. No. 542/GO/Rebi/S/02/CPCSEA) in accordance with CPCSEA guidelines.

2.6. Assessment of anticonvulsant activity

2.6.1. Maximal electroshock seizure (MES) test

The rats divided into six groups. Group 1 (Control) received the vehicle, and group 2 received phenytoin (25 mg/kg i.p.). The synthetic compounds fbnm, **1, 2** and **3** were given to groups 3, 4, 5 and 6 at doses of 10 mg/kg b. w., respectively. All treatments were given to animals 45 min before the test, orally. The 150 mA of current through a corneal electrode (Electro-convulsometer, model no. 100–3) was applied to induce generalized tonic- clonic- seizures in rats. The readings were taken as tonic flexion, tonic extensor phase, stupor, and recovery or death. In generalized tonic-clonic seizures, the reduction in the ratio of tonic extensor phase to flexion (E/F ratio) has been used as a measure of medication efficacy [36].

2.6.2. Pentyleneterazole (PTZ) induced convulsions

In this anticonvulsant model, the rats were divided into six groups, similar to previous model. Group 1 (control) received a vehicle while group 2 received diazepam 4 mg/kg i.p. The compounds fbnm, **1, 2**, and **3** were given to groups 3, 4, 5 and 6 at doses of 10 mg/kg p.o. To induce convulsions, PTZ 50 mg/kg i.p. was administered to the animals. The anticonvulsant activity was measured by delay in onset of a jerk, abolition of convulsion, and protection against PTZ-induced convulsion [37].

2.7. Assessment of anti-anxiety activity

2.7.1. Elevated plus maze test

The anxiolytic and anxiogenic responses of the extract were investigated using the elevated plus maze test. It generates an approach avoidance conflict which is stronger in the open arm compared to the enclosed arm. The anxious rat spent more time in the enclosed arm. The Elevated plus maze consists of two open arms (48.5 × 10 cm) and two close arms (48.5 × 10 × 35.5 cm) with an open roof. The apparatus is elevated to a height of 60.5 cm from the floor. Animals are divided into six groups (six rats in each group). Group 1 (Control) received a vehicle,

Group 2 received Diazepam 2 mg/kg i.p.). The compound, fbnm, **1, 2** and **3**, at doses of 10 mg/kg p.o. were given to groups 3, 4, 5 and 6, respectively. The experiment started 45 min after the rats were given the medication and ended five minutes later. Animals were placed in the central open square facing toward one of the close arms. The number of entries and time spent in closed arms, as well as the number of entries and time spent in open arms, were recorded during the 5-minute test. To be counted, all four paws must be entered into the arms [38,39].

2.7.2. Open field test

An open field test was carried out to determine the anxiolytic action of the compounds on the rats. Animals are divided into six groups (six rats in each group). Group 1 (Control) received a vehicle, Group 2 received Diazepam 2 mg/kg i.p.). The compound fbnm, **1, 2** and **3**, at doses of 10 mg/kg p.o. were given to groups 3, 4, 5 and 6, respectively. The floor of an open field apparatus measured as 60 × 60 cm. The floor is divided into white and black squares of diameter 15 × 15 cm, each. The height of the open field apparatus is 60 cm. The animal was placed in the central region and the activity of all grouped animals was noted for 5 min. The number of squares crossed, time spent in the central region, and central rearing time were noted during the experiment. If the animals spend more time in the central region after taking the medication, it is considered that the test compound or medication has anxiolytic properties [40].

3. Result and discussion

Three new metal complexes **1**–**3** were synthesized with good to excellent yield between 82 % to 85 % by reacting the methanolic solution of the potassium N-(4-fluorobenzyl) N-(naphthalen-1-ylmethyl) dithiocarbamate ligand (fbnm) with the corresponding metal (II) acetate salt [$M(CH_3COO)_2{\cdot}nH_2O$ {M=Ni, Cu, and Zn}] in a molar ratio of 2:1 at room temperature. All the complexes are found air stable and soluble in many organic solvents like dimethyl sulfoxide (DMSO), methanol, ethanol, chloroform, dichloromethane (DCM), *etc*. All compounds were analyzed and characterized by different scientific techniques like FTIR, UV–Vis, NMR, and HRMS. Melting points of ligand was found 295 °C and metal complexes were melted at temperature range 276–206 °C which was primary confirmation of metal-ligand coordination.

3.1. Spectroscopy

3.1.1. FTIR spectroscopy

KBr pellets of each compound were prepared to record their FTIR spectra (Fig. 1) and carefully compared and assigned. Weak absorption bands around 3070–3000 cm^{-1} and 2900–2850 cm^{-1} are observed for C—H vibrations of the aromatic and aliphatic carbons, respectively. The strong absorption bands between 1508 and 1505 cm^{-1} are indicative of the partial C═N of the thioureide while strong absorption bands between 1224 and 1212 cm^{-1} are assigned to the vibration associated with C—N single bond in the thioureide. ν(C—N) in ligand spectrum is present at 1212 cm^{-1} and the same characteristic band is observed around 1224–1222 cm^{-1} with higher frequency shift which denotes development of double bond character between C—N which is supportive of bidentate coordination. The characteristic C-S bond stretching vibration was observed at 1004 cm^{-1} in the ligand spectrum and after complexation the same vibration was observed at higher wavenumber around 1019–1015 cm^{-1} which is clear indication of metal-ligand bonding.

3.1.2. Electronic spectra and magnetic moment

The absorption spectra of ligand fbnm and complexes **1**–**3** were recorded with 10^{-5} M solution of each using DCM:chloroform (50:50) solvent over 200–800 nm range and are shown in Fig. 2. Magnetic moment of complexes was measured with Cahn Faraday electrobalance and values are given in Bohr Magneton (BM). Ligand (fbnm) and complexes **1**–**3** are soluble in mixture of DCM and chloroform, showing an

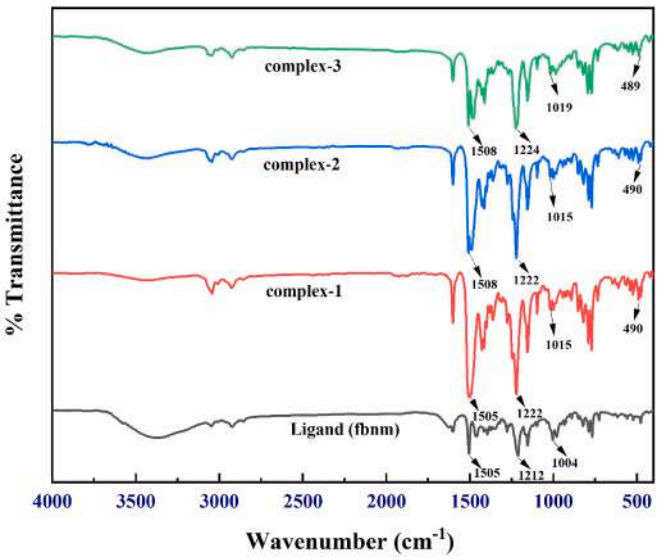

Fig. 1. FTIR spectra of Ligand fbnm and Complexes **1**–**3**.

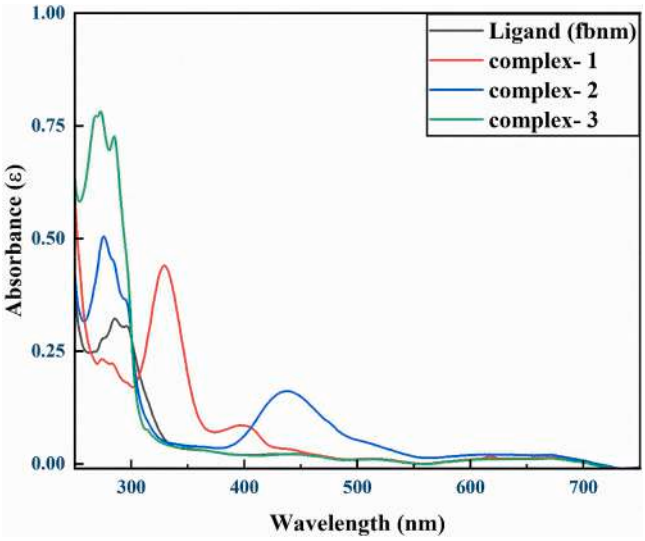

Fig. 2. UV-visible spectra of Ligand fbnm and Complexes **1**–**3**.

absorption band in range 286–272 nm assigned to intra-ligand л→л* transition. The electronic spectrum of complex **1** exhibit three more absorption bands at 330 nm, 400 nm, and 620 nm, where 330 nm band is assigned to metal to ligand charge transfer (MLCT), while 400 and 620 nm bands are due to d-d transitions ($d_{xy}\rightarrow d^2_{xy}$ and $d^2_z\rightarrow d^2_{xy}$ transition) in metal d-orbitals. Diamagnetic behavior of complex **1** with this observed d-d transition are supportive of square planar geometry of the complex **1** around Ni (II) central metal ion. In the spectrum of complex **2**, one intense band at 276 nm is attributed to intra-ligand charge transfer (ILCT) transition mainly associated with N—C═S and S-C═S moieties and a broad absorption band at 440 nm is assigned to the d-d transition for Cu (II) in a square planar geometry. In addition to this d-d transition for complex **2**, the observed μ_{eff} value of 1.74 BM is also supportive of the square planar geometry [41]. Since Zn (II) have d^{10} electronic configuration so electronic spectrum of complex **3** shows only absorption bands at 272 nm and 283 nm which are attributed to л→л* and ILCT transitions [42,43].

3.1.3. ^{1}H NMR spectroscopy

Proton NMR spectra of Ligand fbnm and complexes **1**–**3** were recorded in DMSO-d_6 solvent and the spectra are shown in Fig. S1-S3 respectively. In the ^{1}H NMR spectrum of ligand (fbnm), signals observed between 8.07–7.01 ppm are assigned to aromatic protons, signals found at chemical shift values of 5.75 ppm and 5.33 ppm are attributed to methylene protons of -$CH_2C_{10}H_7$ and -$CH_2C_6H_4F$ moieties, respectively. Upon complexation these chemical shifts values are observed slightly up field which are clearly seen in ^{1}H NMR spectrum of complexes **1** and **3**. Signals for aromatic protons in complexes **1** and **3** are found at 7.95 ppm – 7.09 ppm and 7.98 ppm – 7.09 ppm, respectively. Signals for methylene protons in complexes **1** and **3** are observed at 5.26 ppm and 5.53 ppm for -$CH_2C_{10}H_7$ moiety while 4.75 ppm and 5.53 ppm for -$CH_2C_6H_4F$ moiety, respectively.

3.1.4. ^{13}C NMR spectroscopy

^{13}C NMR spectra of ligand fbnm and complexes **1**–**3** were recorded in DMSO-d_6 and chloroform-*d* solvents and represented in Fig. S4-S6, respectively. In the ^{13}C NMR spectrum of the free ligand fbnm, carbon present in -CS_2 moiety resonated at 217.15 ppm. Upon complexation, the same signal appeared at 207.72 ppm in complex **1** and 208.10 ppm in complex **3**, the up-field shift with respect to that of the ligand could be due to de-shielding of carbon nuclei of -NCS_2 moiety caused by the movement of the electron density from -NCS_2 moiety to the Zn (II) ion. The signals for aromatic carbons of free ligands were observed in the range 162.46 ppm to 115.03 ppm while the signals for the same carbons of complexes were found between 162.49 −115.31 ppm for complex **1** and 163.02–115.70 ppm for complex **3** with slightly down-field shifts. Methylene carbons of $CH_2C_{10}H_7$ and -$CH_2C_6H_4F$ moieties in the ligand (fbnm) were resonated at 53.31 ppm and 52.59 ppm, however, upon complexation the same signals were found at 51.08 ppm and 50.01 ppm for complex **1** while at 56.59 ppm and 55.67 ppm for complex **3**, respectively. Overall, no significant changes were seen in the chemical shift values of aromatic and methylene carbons upon complexation which indicates that these carbons do not participate in the bond formation during complexation.

3.1.5. Mass spectroscopy

Ligand fbnm and all complexes **1**–**3** were also investigated through high resolution mass spectroscopy to confirm their formation with determination of their molecular weight by observing their molecular ion peaks in their mass spectra (Fig. S7-S10). The molecular ion peak $[M]^+$ of the ligand (fbnm) was found at *m/z* 379.0342 which is very much concordant with its calculated *m/z* value 379.0267. Similarly, $[M+H]^+$ peak for each of the complexes **1**–**3** was found in their mass spectra at *m/z* 739.0690, 744.0621, and 745.0597 which are in good agreement with their calculated *m/z* values 739.0687, 744.0629, and 745.0625, respectively.

3.2. Thermogravimetric analysis (TGA)

The thermal decomposition of complexes **1**–**3** was investigated under nitrogen atmosphere from temperature 30 °C to 700 °C and their weight loss percentage with increment of temperature were depicted in Fig. 3. From the obtained data, it was observed that all the three metal complexes were thermally decomposed into metal sulfides with two steps decompositions. First step of decomposition was observed between 120 and 340 °C for all complexes which correspond to loss of aromatic ring moieties while the second step of decomposition was seen after 340 °C with loss of NCS moiety resulting the formation of metal sulfides. For complex **1**, a total weight loss of 88.765% was observed in temperature range 30–340 °C which was indicative for elimination of water, aromatic ring moieties and NCS moiety (calcd. 88.01 %). The thermal decomposition of complex **1** was finished at 700 °C with the formation of NiS (found 11.235 %, calcd. 11.988 %). Further, the complex **2** and **3** were also thermally decomposed into CuS (found 7.989 %, calcd. 12.842 %) and ZnS (found 13.073 %, calcd. 13.056 %), respectively where the first step of decomposition involved the elimination of organic ring moieties (found 83.192 %, calcd. 79.356 %) for complex **2** and (found 79.732 %, calcd. 79.161 %) for complex **3** while the second step of decomposition finished with the elimination of NCS moiety with loss of 8.819% and 7.195 % for complex **2** (calcd. 7.801 %) and complex **3** (calcd. 7.782 %), respectively.

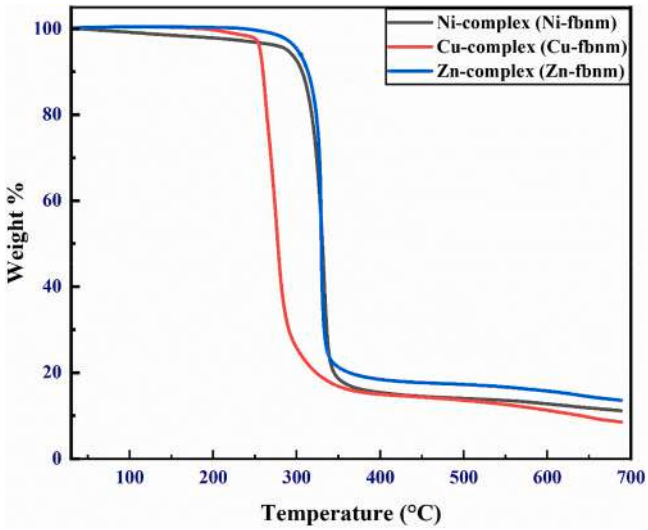

Fig. 3. TGA plot of Ligand complexes **1**–**3**.

3.3. Crystal structure description

3.3.1. Complex 2

Fig. 4 shows the ORTEP diagram of the complex **2** along with the atom numbering scheme. The structural refinement data related to complex **2** is listed in Table 1 and the selected bond distances and bond angles are presented in Table 2. In complex **2**, the Cu(II) ion is coordinated *via* four dithio sulfur atoms of two moieties of ligands. The CuS_4 core displays a distorted square planar geometry around the Cu(II) ion. All Cu–S bond lengths are slightly unequal and lie between 2.297(3)-2.303(3) Å. The bite angles found between two metal chelate rings are slightly diverse {S(4)-Cu(1)-S(3) = 77.56(10) and S(2)-Cu(1)-S(1) = 77.24(10)°} and less than reported normal bond angle (90°) which suggest that the complex have distorted square planar geometry [44]. The other bond angles viz. S(2)-Cu(1)-S(3) and S(4)-Cu(1)-S(1) are 102.54(11) and 102.67(11)°, respectively which also suggest the deviation from a regular square planar geometry around the Cu(II) ion. The nitrogen and carbon (C—N) bond lengths of the two NCS_2 moieties of the dithiocarbamate ligands{N(1)-C(1) = 1.275(13) and N(2)-C(20) = 1.315(12) Å} are shorter than the normal single N–C bond length credited to the partial double bond character and indicates the delocalization of the π-electrons in the NCS_2 moiety of the ligand [45]. The crystal structure of complex **2** is stabilized by weak C–H···F intermolecular interactions found between C–H hydrogen of the biphenyl ring and fluorine atom of the nearby bi-phenyl ring (Fig. S11).

3.3.2. Complex 3

Fig. 5 shows the ORTEP diagram of complex **3** with the atomic numbering schemes. The structural refinement data related to complex **3** is listed in Table 1 and the selected bond distances and bond angles are presented in Table 3. Complex **3** comprises one independent asymmetric dinuclear unit. Complex **3** consists of two tetrahedral Zn(II) centres, each center coordinated through two dithiocarbamato ligands moieties. Out of the four dithioligands moieties, two ligands act as uni-negative chelating bidentate manner whereas the other two units as bridging bidentate coordinated to two Zn(II) centers, creating an eight-membered

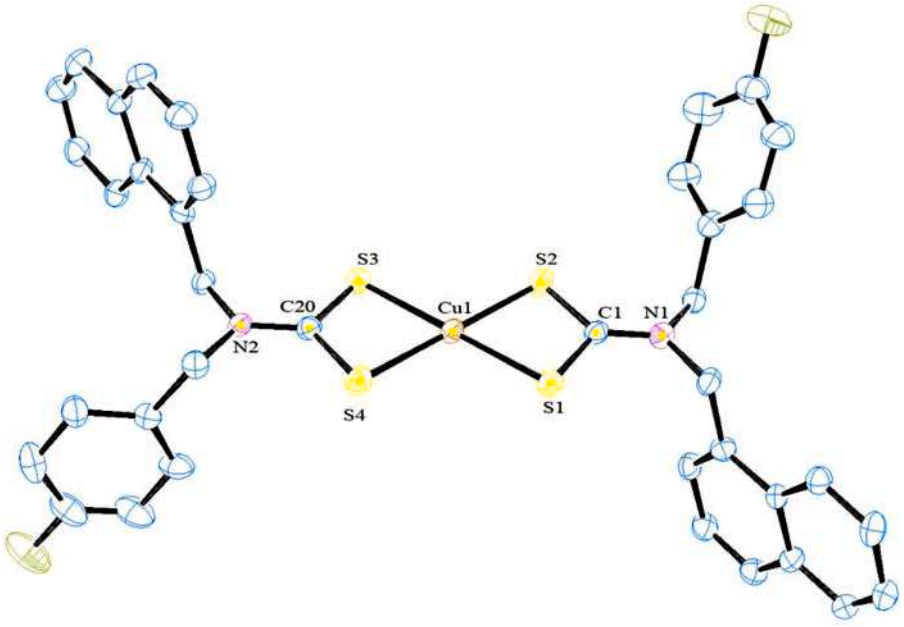

Fig. 4. ORTEP diagram of Cu(II) complex (**2**) at 20% probability level. Hydrogen atoms are omitted for clarity.

Table 1
Crystallographic data of complexes **2** and **3**.

Parameters	2	3
Empirical formula	$C_{38}H_{30}F_2N_2S_4Cu$	$C_{38}H_{30}F_2N_2S_4Zn$
Molecular weight	744.42	746.25
Crystal system	Monoclinic	Monoclinic
Space group	*P 21*	*P 21/n*
T (K)	100(2)	293 (2)
λ, Mo Kα (Å)	0.71073	0.71073
a (Å)	7.5407(2)	10.4967(2)
b (Å)	20.9057(5)	10.4099(4)
c (Å)	11.0577(2)	32.1775(9)
α (°)	90	90
β (°)	105.386(2)	91.796(2)
γ(°)	90	90
V, (Å^3)	1680.70(7)	3514.29(18)
Z	2	4
ρ_{calcd} (g/cm^3)	1.471	1.410
μ (mm^{-1})	3.585	3.523
F(000)	766	1536
Crystal size (mm)	0.27 × 0.21 × 0.14	0.24 × 0.20 × 0.14
θ range for data collections(°)	4.146 to 72.296	2.748 to 72.366
Index ranges	−9<=h<=9, −25<=k<=25, −10<=l<=13	−9<=h<=12, −12<=k<=12, −39<=l<=39
No. of reflections collected	33,986	24,498
No. of independent reflections(R_{int})	6583 (0.0591)	6856 (0.0419)
No. of data/restrains/parameters	6583 / 1 / 425	6856 / 0 / 424
Goodness-of-fit on F^2	1.184	1.056
R_1^a, wR_2^b [(I>2σ(I)]	0.1085, 0.2607	0.0530, 0.1270
R_1^a, wR_2^b (all data)	0.1179, 0.2756	0.0788, 0.1502
Largest difference in peak /hole (e. Å^{-3})	3.530 and −0.532	0.504 and −0.405
CCDC	2291494	2281316

$^a R_1 = \Sigma||F_o| - |Fc||\Sigma|F_o|$.
$^b R_2 = [\Sigma w(|F_o^2| - |F_c^2|)^2/\Sigma w|F_o^2|^2]^{1/2}$.

Table 2
Bond length (Å) and angles (°) for Complex **2**.

Bond length (Å)		Bond angle (°)	
Cu(1)-S(4)	2.297(3)	S(4)-Cu(1)-S(2)	179.20(14)
Cu(1)-S(2)	2.297(3)	S(4)-Cu(1)-S(3)	77.56(10)
Cu(1)-S(3)	2.300(3)	S(2)-Cu(1)-S(3)	102.54(11)
Cu(1)-S(1)	2.303(3)	S(4)-Cu(1)-S(1)	102.67(11)
S(1)-C(1)	1.751(11)	S(2)-Cu(1)-S(1)	77.24(10)
S(2)-C(1)	1.727(9)	S(3)-Cu(1)-S(1)	179.73(13)
S(3)-C(20)	1.731(11)	C(1)-S(1)-Cu(1)	85.4(3)
S(4)-C(20)	1.723(10)	C(1)-S(2)-Cu(1)	86.1(4)
F(1)-C(6)	1.365(16)	C(20)-S(3)-Cu(1)	84.6(3)
F(2)-C(25)	1.354(16)	C(20)-S(4)-Cu(1)	84.9(4)
N(1)-C(1)	1.275(13)	C(1)-N(1)-C(9)	123.4(9)
N(1)-C(9)	1.455(13)	C(1)-N(1)-C(2)	121.5(9)
N(1)-C(2)	1.473(14)	C(9)-N(1)-C(2)	114.7(9)
N(2)-C(20)	1.315(12)	N(1)-C(1)-S(2)	125.1(8)
N(2)-C(28)	1.467(12)	N(1)-C(1)-S(1)	123.7(7)
N(2)-C(21)	1.474(14)	S(2)-C(1)-S(1)	111.3(6)

ring having Zn(1)-S(3)-C(12)-S(4)-Zn(1)-S(3)-C(12)-S(4) atoms. In this way complex **3**, involves an eight-membered cyclic core ($Zn_2S_4C_2$) with an approximate chair-like structure, in which the atoms Zn(1)-S(4)-C (12)-S(3) form the base of the chair while the others S(4) and Zn(1) atoms lie out of the plane formed by this base in a plane that is almost perpendicular to it. The angles found around the zinc atoms are S(4)-Zn (1)-S(2) = 112.71(4)°, and S(1)-Zn(1)-S(2)= 74.84(3)° which suggest a distorted tetrahedral geometry around both zinc centers in complex **3** [46–48]. The dihedral angles between the planes of these all chelate rings are 54.31°. Two dithiocarbamato ligands are bonded to each Zn(II) ions in a chelating-bridging manner which generates a dimer complex with distorted tetrahedral coordination geometry around both Zn(II) centers. The Zn(1)-S(4), Zn(1)-S(1) and Zn(1)-S(2) bond distances (2.3367(11), 2.3534(10), and 2.4745(10) Å are shorter than the Zn(1)-S (3) bond lengths (2.7351(10) Å which indicate that all three sulfur atoms (S1, S2, and S3) are coordinated through Zn(II) ions, however, S (3) atom is attached through interaction (not coordinated). In the solid state, the complex is stabilized via intermolecular C—H···F interactions between fluorine atoms of the phenyl ring and CH hydrogen atoms of the CH_2 attached to the phenyl ring of the nearby other molecules and naphthyl rings leading to a ladder-like arrangement (Fig. S12). In addition, the structure of complex **3** is also stabilized by C—H···π (2.542 Á) interactions between CH hydrogen of the fluorophenyl ring and π electrons of the metal chelate ring (Fig. S13).

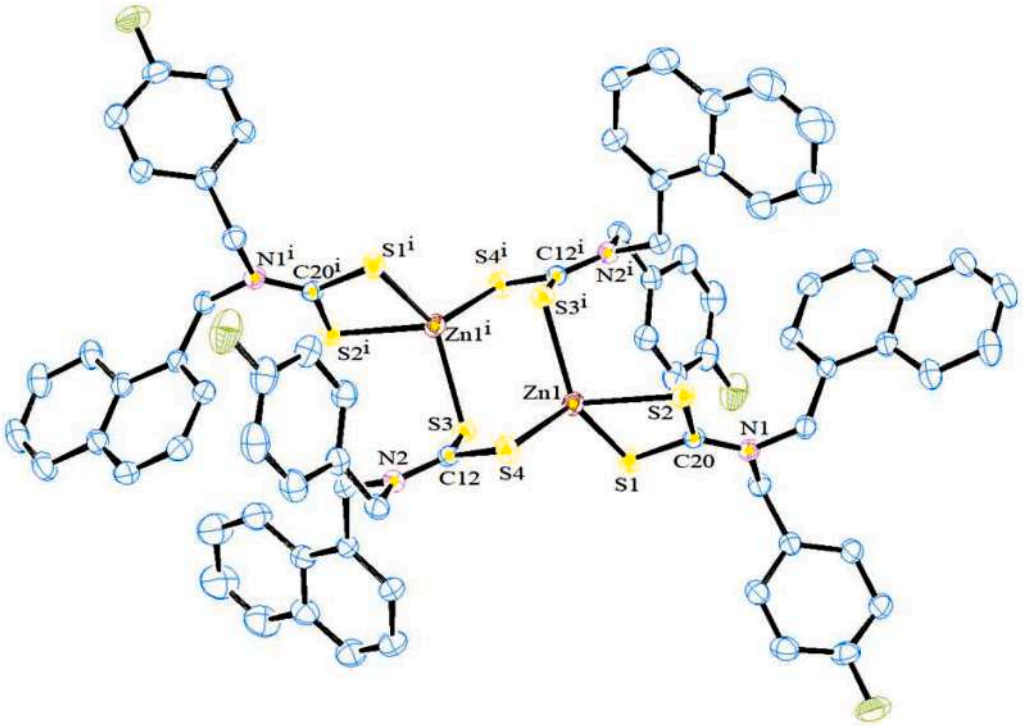

Fig. 5. ORTEP diagram of Zn(II) complex (**3**) at 20% probability level. Hydrogen atoms are omitted for clarity.

Table 3
Bond length (Å) and angles (°) for Complex **3**.

Bond length (Å)		Bond angle (°)	
Zn(1)-S(4)	2.3367(11)	S(4)-Zn(1)-S(1)	123.34(4)
Zn(1)-S(1)	2.3534(10)	S(4)-Zn(1)-S(3)#1	103.64(4)
Zn(1)-S(3)#1	2.4112(10)	S(1)-Zn(1)-S(3)#1	130.95(4)
Zn(1)-S(2)	2.4745(10)	S(4)-Zn(1)-S(2)	112.71(4)
Zn(1)-S(3)	2.7351(10)	S(1)-Zn(1)-S(2)	74.84(3)
S(3)-C(12)	1.733(4)	S(3)#1-Zn(1)-S(2)	101.07(3)
S(2)-C(20)	1.715(3)	S(4)-Zn(1)-S(3)	71.03(3)
S(1)-C(20)	1.733(4)	S(1)-Zn(1)-S(3)	93.62(3)
S(4)-C(12)	1.714(4)	S(3)#1-Zn(1)-S(3)	88.58(3)
N(2)-C(12)	1.323(4)	C(12)-S(3)-Zn(1)#1	103.97(11)
N(1)-C(20)	1.322(4)	C(12)-S(3)-Zn(1)	78.70(12)
F(1)-C(16)	1.360(5)	Zn(1)#1-S(3)-Zn(1)	91.41(3)
F(2)-C(25)	1.370(6)	C(12)-S(4)-Zn(1)	91.63(13)

Symmetry transformations used to generate equivalent atoms: #1 -x+1,-y+1,-z+1

3.4. Assessment of anticonvulsant activity

3.4.1. MES test

The synthetic compounds, fbnm, **1, 2** and **3** decreased the duration of hind limb extension significantly in all groups of treatment compared to the control group. The duration of flexion was reduced in all treatment groups compared to the control group, but the compound **2** and **3** significantly reduced the duration of flexion after treatment. The duration of extensor also get reduced in all groups but significant results were obtained in case of compound **1**. The extensor and flexion were completely abolished in the groups of phenytoin. Whereas clonus phase was found to be non- significant in all treatment groups ($p > 0.05$) compared to the control group except for the phenytoin group ($p < 0.05$). The stupor phase was also significantly ($p < 0.05$) reduced in compounds fbnm, **3** and phenytoin (Fig. 6, Table 4).

3.4.2. PTZ induced convulsions

In all treatment groups, synthetic compounds delayed the onset of PTZ -induced myoclonic jerks. The onset of convulsion was most significantly delayed by 92 s when complex **3** was administered at a dose of 10 mg/kg b. w., compared to 48 s in the control group. The duration of jerks in all the treatment groups were found non-significantly ($p > 0.0001$) compared to the control group. The onset of clonus was delayed by 688 ± 47 s in the fbnm group, compared to 186 ± 16.64 s ($p < 0.001$) in the control group, whereas the other groups (diazepam and complex **2**) recovered and no clonus phase was detected. The onset of extensor was not observed in diazepam and complex **2** and the results obtained were significant ($p < 0.001$) in all groups when compared with control group. In all treatment groups, no incidence of mortality was recorded, whereas in the control group treated with a vehicle, 50 % mortality was recorded (Fig. 7, Table 5).

3.5. Effect on anxiety

3.5.1. Elevated plus maze

The Elevated plus maze test showed a decrease in the number of entries in the open arm and close arm both in all the treatment groups but the results obtained were non-significant. The time spent in close arm by all the treated groups with fbnm, **1, 2** and **3** did not differ significantly from the control group. On the other hand, time spent in the open arm by the treated groups did not differ significantly from the control group, but time spent in the open arm by the diazepam treated group increased significantly (Fig. 8, Table 6).

3.5.2. Open field test

The doses of synthetic compounds fbnm, **1, 2, 3** and diazepam were given to the separate groups of rats. The number of squares crossed by all treatment groups decreased significantly ($p < 0.001$–0.01) compared to the control groups. The number of central area rearing was increased in all groups but not significantly ($p > 0.05$) compared to the control group, except for the diazepam group ($p < 0.01$). The time spent in the central area did not change significantly ($p > 0.05$) in any of the treatment

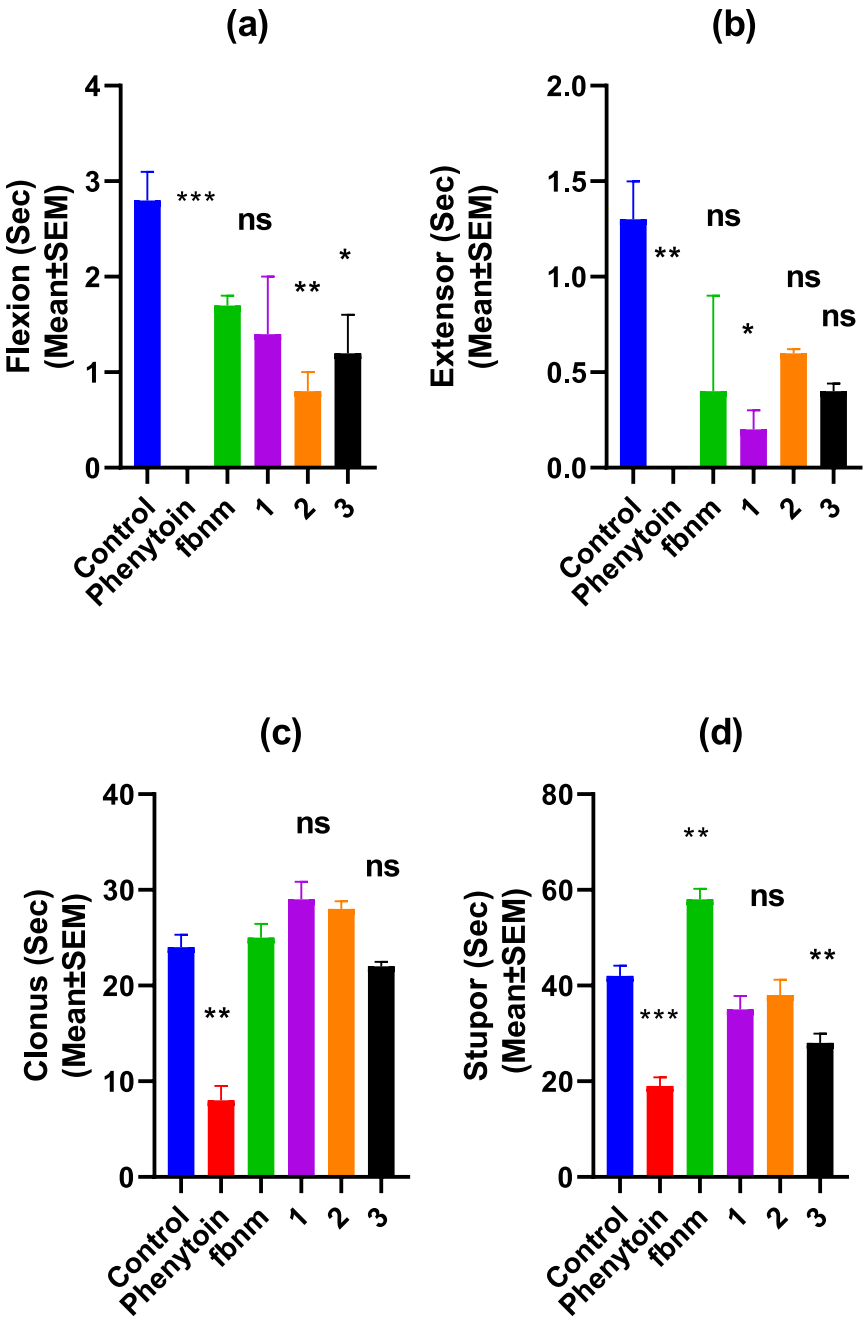

Fig. 6. Anticonvulsant study of fbnm and different compounds (1, 2 and 3) via Maximal electroshock seizure model, (a): Flexion (sec), (b): Extensor (sec), (c): Clonus (sec), (d): Stupor (sec), *Values are expressed as Mean ± SEM (n = 6). *Denotes statistically significant values (One Way ANOVA followed by Dunnett Post Test) relative to control group (ns=non-significant; ****= $p < 0.0001$, ***= $p < 0.001$, **= $p < 0.01$ and *= $p < 0.1$).*

Table 4
Anticonvulsant activity of different compounds during MES model.

Groups	Flexion (Sec)	Extensor (Sec)	Clonus (Sec)	Stupor (Sec)
Control	2.8 ± 0.3	1.3 ± 0.2	24 ± 1.3	42 ± 2.15
Phenytoin	0 ± 0	0 ± 0	8 ± 1.5	19 ± 1.85
Ligand (fbnm)	1.7 ± 0.1	0.4 ± .5	25 ± 1.45	58 ± 2.24
Complex **1**	1.4 ± 0.6	0.2 ± 0.01	29 ± 1.86	35 ± 2.84
Complex **2**	0.8 ± 0.2	0.6 ± 0.02	28 ± 0.8	38 ± 3.2
Complex **3**	1.2 ± 0.01	0.4 ± 0.04	22 ± 0.47	28 ± 1.94

#Values expressed as mean ± SEM. Significant difference from control, $p < 0.05$.

groups, while time spent in the central area increased significantly ($p < 0.001$) in the diazepam group compared to the control group (Fig. 9, Table 7).

Both MES and PTZ-induced convulsions models are the major pharmacological screening models for the evaluation of any therapeutic agent to be approved for its clinical significance. During MES model, the parameters like flexion, extensor, clonus and stupor represent the onset of convulsions and their delayed action indicate the therapeutic application by any synthetic agent. During the study of this model it was concluded that there was a delayed response of complex **2** for both flexion and extensor whereas delayed response of stupor for complex **3**

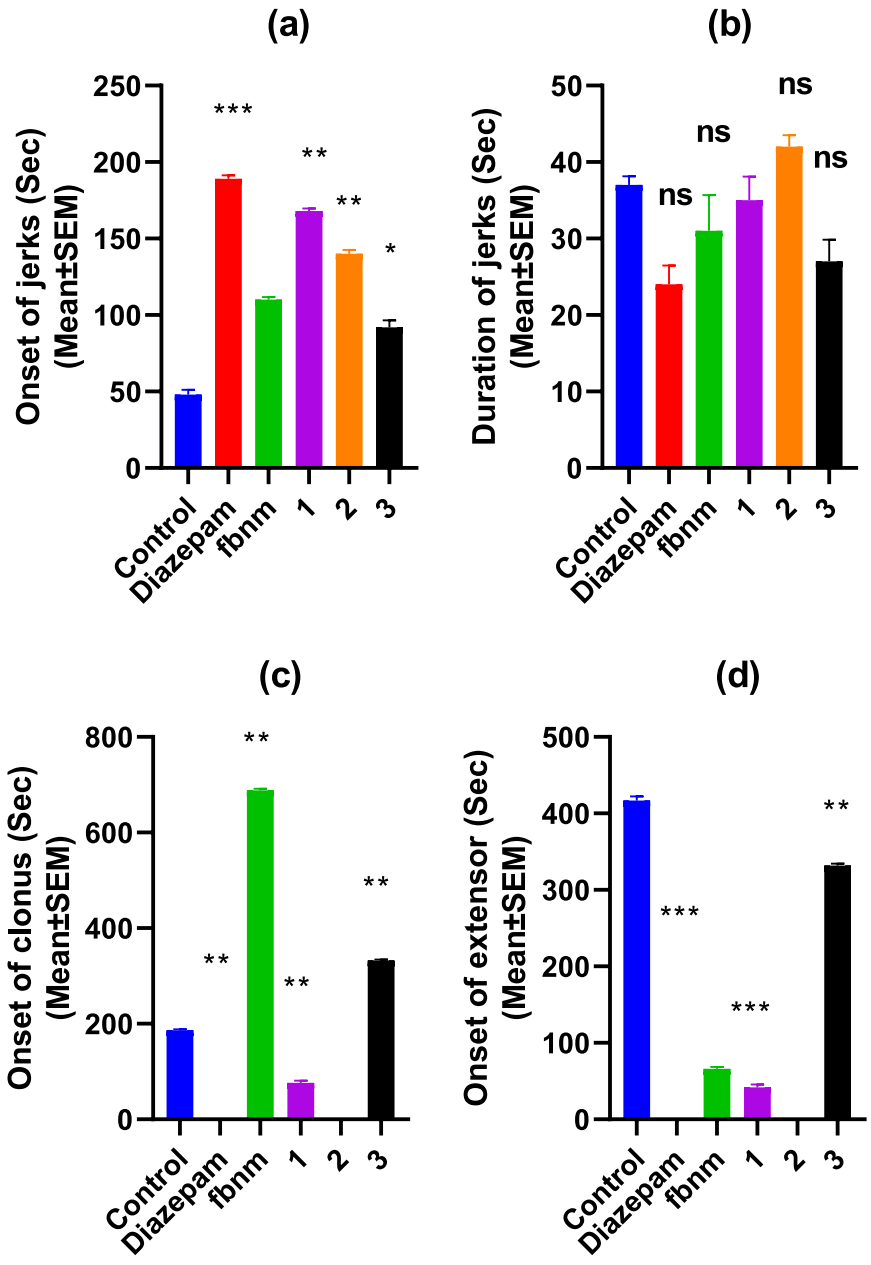

Fig. 7. Anticonvulsant study of fbnm and different compounds (1, 2 and 3) via Pentyleneterazole model, (a): Onset of jerks (sec), (b): Duration of jerks (sec), (c): Onset of clonus (sec), (d): Onset of extensor (*sec*), *Values are expressed as Mean ± SEM (n = 6).*Denotes statistically significant values (One Way ANOVA followed by Dunnett Post Test) relative to control group (ns=non-significant; ****= $p < 0.0001$, ***= $p < 0.001$, **= $p < 0.01$ and *= $p < 0.1$).*

Table 5
Anticonvulsant activity of different compounds during PTZ model.

Groups	Onset of jerks (Sec)	Duration of jerks (Sec)	Onset of clonus (Sec)	Onset of extensor (Sec)
Control	48 ± 3.21	37 ± 1.15	186 ± 2.15	417 ± 5.16
Diazepam	189 ± 2.45	24 ± 2.48	0 ± 0	0 ± 0
Ligand (fbnm)	110 ± 1.86	31 ± 4.69	688 ± 3.56	66 ± 2.58
Complex **1**	168 ± 1.79	35 ± 3.12	76 ± 5.14	42 ± 3.54
Complex **2**	140 ± 2.54	42 ± 1.54	0 ± 0	0 ± 0
Complex **3**	92 ± 4.49	27 ± 2.87	332 ± 2.48	339 ± 2.49

#Values expressed as mean ± SEM. Significant difference from control, $p < 0.05$.

and fbnm. The MES-induced epilepsy model screens antiepileptic compounds which act by blocking voltage-dependent Na^+ channels.

In the second anticonvulsant model the onset of jerks, duration of jerks onset of clonus and onset of extensor are major parameters which control the mechanism of convulsion during its occurrence. During this model it was concluded that the onset of jerks, onset of clonus and onset of extensor was significantly reduced by the complexes **1** and **2**. These findings suggest that these compounds were very efficient in abolishing PTZ-induced seizures.

The effect of a medicine on animals with PTZ-induced epilepsy can be used to evaluate its impact on generalized absence seizures. Diazepam (benzodiazepines) is a GABA facilitator, whereas PTZ is a $GABA_A$ receptor antagonist. This suggests that the anticonvulsant effect of complexes **1** and **2** against PTZ-induced seizures is mediated by the GABA-chloride channel.

The elevated plus maze test was based on the fear of balancing on a

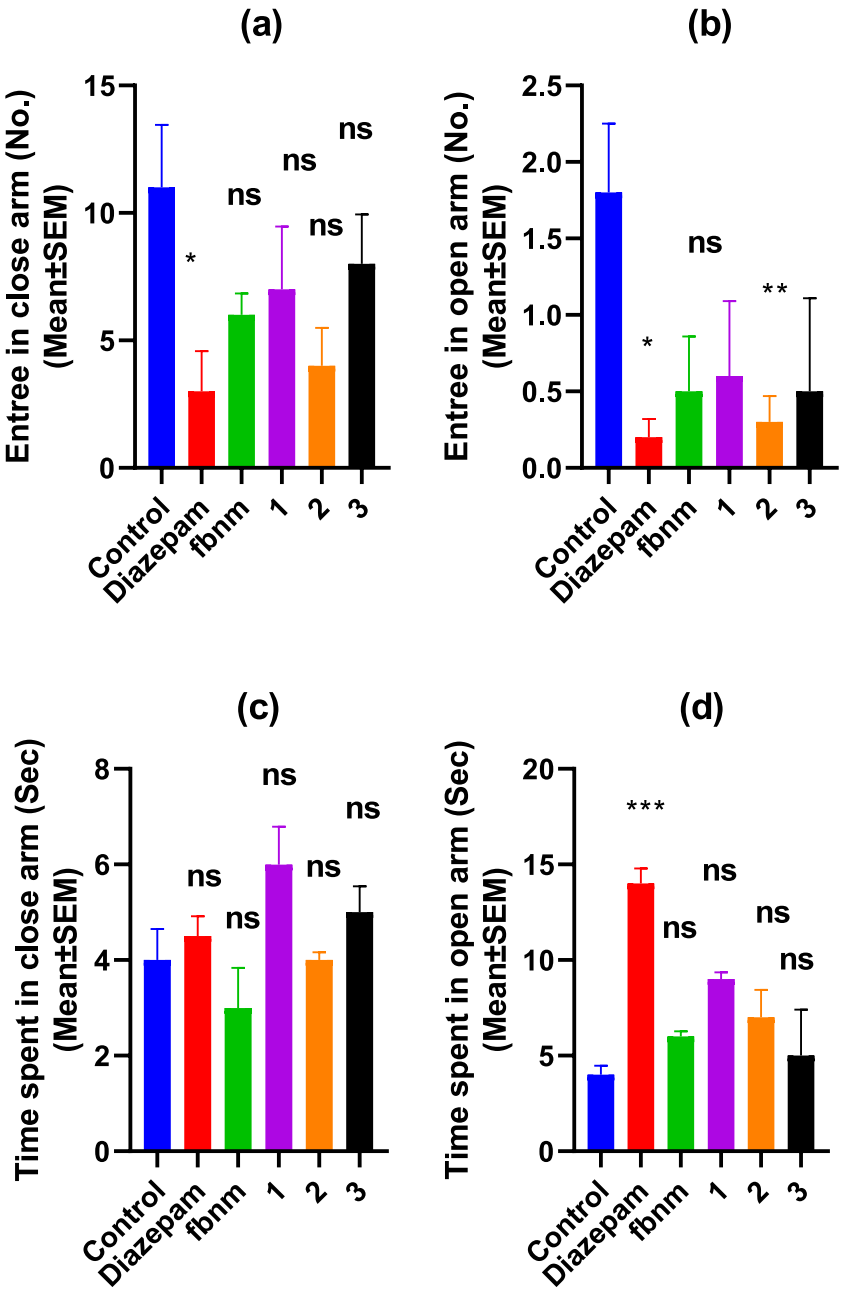

Fig. 8. Antianxiety study of fbnm and different compounds (1, 2 and 3) via Elevated plus maze test., (a): Entrée in close arm (No.), (b): Entrée in open arm (No.), (c): Time spent in close arm (sec), (d): Time spent in open arm (sec), *Values are expressed as Mean ± SEM (n = 6).*Denotes statistically significant values (One Way ANOVA followed by Dunnett Post Test) relative to control group (ns=non-significant; ****= $p < 0.0001$, ***= $p < 0.001$, **= $p < 0.01$ and *= $p < 0.1$).*

Table 6
Antianxiety activity of different compounds during elevated plus maze model.

Groups	Entrée in close arm (No.)	Entrée in open arm (No.)	Time spent in close arm (Sec)	Time spent in open arm (Sec)
Control	11 ± 2.46	1.8 ± 0.45	4 ± 0.65	4 ± 0.48
Diazepam	3 ± 1.58	0.2 ± 0.02	4.5 ± 0.42	14 ± 0.79
Ligand (fbnm)	6 ± 0.85	0.5 ± 0.06	3 ± 0.84	6 ± 0.28
Complex **1**	7 ± 2.47	0.6 ± 0.09	6 ± 0.79	9 ± 0.36
Complex **2**	4 ± 1.49	0.3 ± 0.07	4 ± 0.16	7 ± 1.45
Complex **3**	8 ± 1.94	0.5 ± 0.01	5 ± 0.54	5 ± 2.4

Values expressed as mean ± SEM. Significant difference from control, $p < 0.05$.

narrow space and the aversion to unexpected open spaces. As a result, avoiding open arms is regarded as an anxious behaviour. Anxiolytic medicines like diazepam, increase the time and number of entries into the open arms. The time spent in the open arm by the fbnm, **1, 2** and **3** treated groups was not significantly different from the control group, but diazepam-treated groups spent more time in the open arm. According to these findings, fbnm, **1, 2** and **3** did not influence anxiety via this model.

In an animal test model, an open field was used to examine anxiety behavior. An open field test is used to objectively assess the emotionality of rats. The total number of square crossings utilised to calculate the animal's locomotor activity throughout the experiment. The number of square crossed, time spent in the central area and central area rearing are the parameters that represent the anxious behavior of animals during the study. So only significant results were obtained in case of number of squares crossed for all the tested compounds. These findings indicate

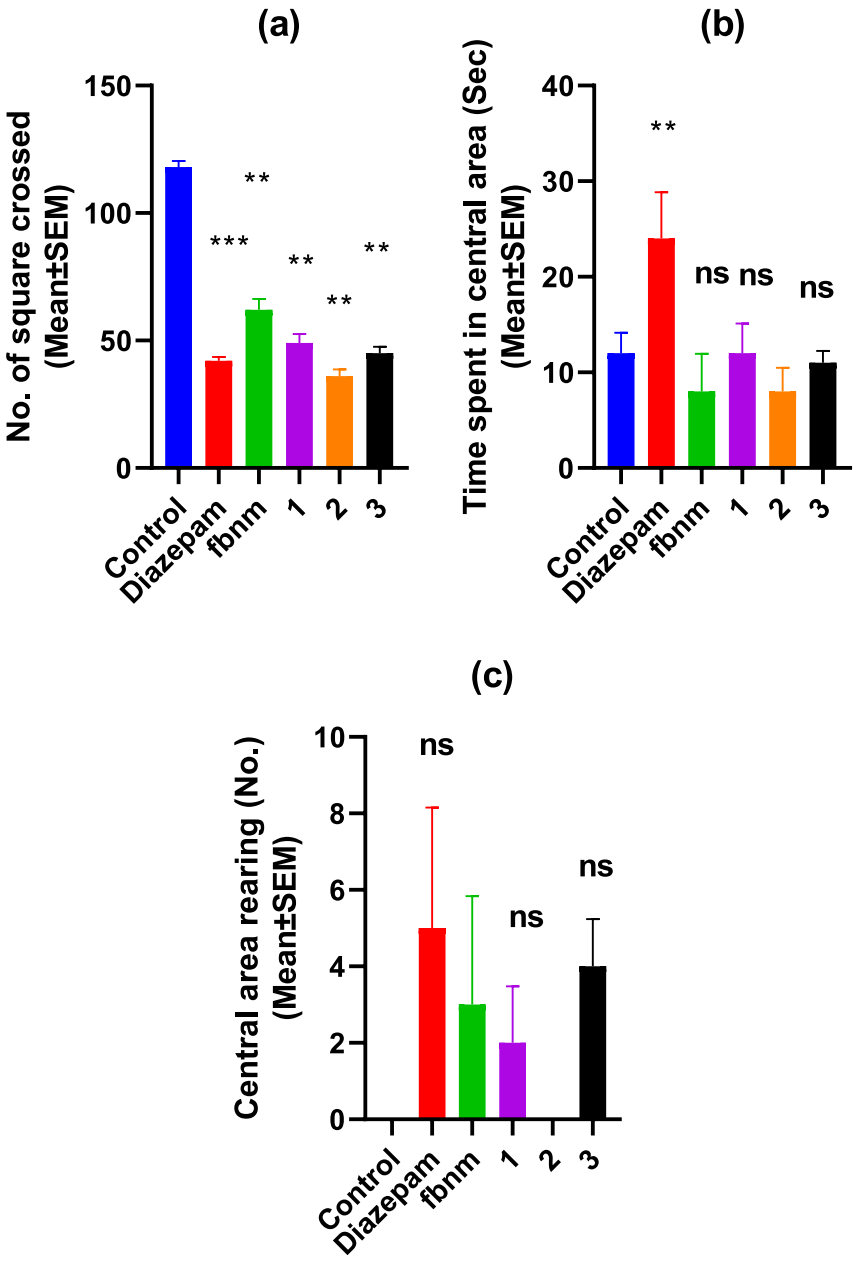

Fig. 9. Antianxiety study of fbnm and different compounds (**1, 2** and **3**) via Open field test, (a): No. of square crossed, (b): Time spent in central area (sec), (c): Central area rearing (No.), *Values are expressed as Mean ± SEM (n = 6).*Denotes statistically significant values (One Way ANOVA followed by Dunnett Post Test) relative to control group (ns=non-significant; ****= $p < 0.0001$, ***= $p < 0.001$, **= $p < 0.01$ and *= $p < 0.1$).*

Table 7
Antianxiety activity of different compounds during elevated open field test.

Groups	Number of square crossed (No.)	Time spent in central area (Sec)	Central area rearing (No.)
Control	118 ± 2.45	12 ± 2.15	0 ± 0
Diazepam	42 ± 1.56	24 ± 4.86	5 ± 0.15
Ligand (fbnm)	62 ± 4.25	8 ± 3.95	3 ± 0.84
Complex **1**	49 ± 3.54	12 ± 3.12	2 ± 0.48
Complex **2**	36 ± 2.65	8 ± 2.47	0 ± 0
Complex **3**	45 ± 2.57	11 ± 1.25	4 ± 0.24

Values expressed as mean ± SEM. Significant difference from control, $p < 0.05$.

that treatment with these synthetic compounds did not have major effect of reducing anxiety.

4. Conclusion

In this work, we have synthesized a 4-fluorobenzyl and naphthalen-1-ylmethyl functionalized ligand (fbnm) and its [Ni(fbnm)$_2$] (**1**), [Cu(fbnm)$_2$] (**2**), and [Zn(fbnm)$_2$] (**3**) complexes. Uv-vis spectra show d-d transitions for complexes **1** and **2** at 620–400 nm range which suggest the square planar geometry around Ni(II) and Cu(II) ions. Further, SCXRD data of complexes **2** and **3** confirms their molecular structures and geometry. The CuS_4 core displays a distorted square planar geometry of complex **2** around the Cu(II) ion due to unequal C-S bond lengths, whereas complex **3** comprises one independent asymmetric dinuclear unit which consists of two tetrahedral Zn(II) centres. The crystal structures of complexes **2** and **3** are stabilized by various weak interactions

generating supramolecular architecture. The thermal decomposition of all the metal complexes was analysed by TG-DTA technique which showed strong evidence for the formation of their respective metal sulfide as the final thermally stable chemical entities.

The in vivo study for potential anti-convulsant and anti-anxiety activities of ligand and complexes were performed. The result revealed that among the ligand and complexes **1**–**3**, complex **2** showed significant anti-convulsant activity because it significantly delayed the onset of clonus and extensor when PTZ was used to induce seizures. On the other hand, all these synthesized compounds did not show significant anti-antianxiety effect. Consequently, the complex **2** may be used as a potential anticonvulsant agent in the future by further biochemical or neurotransmitter estimations to control the onset of generalized tonic-clonic seizures.

Supplementary Material

Crystal data informations of complexes **2** and **3** have been deposited at Cambridge Crystallographic Data Center and their CCDC deposition no. are 2291494 and 2281316, respectively. Copies of the data can be obtained free of charge from the CCDC, Union Road, Cambridge CB1 1EZ, UK (Tel: (+44) 1223-336-408; Fax: (+44) 1223- 336-003; Email: deposit@ccdc.cam.ac.uk).

CRediT authorship contribution statement

Anupam Singh: Conceptualization, Methodology, Data curation, Formal analysis, Visualization, Writing – original draft. **Rajesh Kumar:** Data curation, Software, Investigation, Formal analysis, Writing – original draft. **Kunal Shiv:** Data curation, Software, Formal analysis, Writing – original draft. **Shivendra Kumar Pandey:** Data curation, Software, Formal analysis, Writing – original draft. **M.K. Bharty:** Data curation, Software, Writing – review & editing, Validation. **R.J. Butcher:** Data curation, Software, Validation, Writing – review & editing. **Lal Bahadur Prasad:** Supervision, Resources, Methodology, Investigation, Formal analysis, Validation, Writing – review & editing, Project administration, Funding acquisition.

Declaration of Competing Interest

The authors declare that they have no known competing financial interests or personal relationships that could have appeared to influence the work reported in this paper.

Data availability

Data will be made available on request.

Acknowledgements

Lal Bahadur Prasad and M. K. Bharty gratefully acknowledge Banaras Hindu University, Varanasi for IoE Dev. Scheme No.6031 for financial assistance. Anupam Singh and Kunal Shiv are also acknowledging the University Grant Commission (UGC), New Delhi for financial assistance in the form of a Senior Research Fellow, Ref No.: 3496/(NET-DEC 2018), and Ref No.: 190510635704, respectively.

Supplementary materials

Supplementary material associated with this article can be found, in the online version, at doi:10.1016/j.molstruc.2023.137052.

References

[1] B.L. Nye, V.M. Thadani, Migraine and epilepsy: review of the literature, Headache: J. Head Face Pain 55 (2015) 359–380.
[2] E. Giourou, A. Stavropoulou-Deli, A. Giannakopoulou, G.K. Kostopoulos, M. Koutroumanidis, Introduction to epilepsy and related brain disorders, in: N. S. Voros, C.P. Antonopoulos (Eds.), Cyberphysical Systems for Epilepsy and Related Brain Disorders: Multi-Parametric Monitoring and Analysis for Diagnosis and Optimal Disease Management, Springer International Publishing, Cham, 2015, pp. 11–38, https://doi.org/10.1007/978-3-319-20049-1_2.
[3] J. Liu, P. Zhang, Q. Zou, J. Liang, Y. Chen, Y. Cai, S. Li, J. Li, J. Su, Q. Li, Status of epilepsy in the tropics: an overlooked perspective, Epilepsia Open 8 (2023) 32–45, https://doi.org/10.1002/epi4.12686.
[4] W. Löscher, P. Klein, The pharmacology and clinical efficacy of antiseizure medications: from bromide salts to cenobamate and beyond, CNS Drugs 35 (2021) 935–963, https://doi.org/10.1007/s40263-021-00827-8.
[5] C.J. Landmark, S.I. Johannessen, P.N. Patsalos, Therapeutic drug monitoring of antiepileptic drugs: current status and future prospects, Expert Opin. Drug Metab. Toxicol. 16 (2020) 227–238, https://doi.org/10.1080/17425255.2020.1724956.
[6] W. Löscher, H. Potschka, S.M. Sisodiya, A. Vezzani, Drug resistance in epilepsy: clinical impact, potential mechanisms, and new innovative treatment options, Pharmacol. Rev. 72 (2020) 606–638, https://doi.org/10.1124/pr.120.019539.
[7] K.D. Mjos, C. Orvig, Metallodrugs in Medicinal Inorganic Chemistry, Chem. Rev. 114 (2014) 4540–4563, https://doi.org/10.1021/cr400460s.
[8] M. Kumar, G. Kumar, A. Kant, D.T. Masram, Role of metallodrugs in medicinal inorganic chemistry. Advances in Metallodrugs, John Wiley & Sons, Ltd, 2020, pp. 71–113, https://doi.org/10.1002/9781119640868.ch3.
[9] I. Yousuf, M. Bashir, Metallodrugs in medicine. Advances in Metallodrugs, John Wiley & Sons, Ltd, 2020, pp. 1–39, https://doi.org/10.1002/9781119640868.ch1.
[10] M. Sylla-Iyarreta Veitía, F. Dumas, G. Morgant, J.R.J. Sorenson, Y. Frapart, A. Tomas, Synthesis, structural analysis and anticonvulsant activity of a ternary Cu (II) mononuclear complex containing 1,10-phenanthroline and the leading antiepileptic drug valproic acid, Biochimie 91 (2009) 1286–1293, https://doi.org/10.1016/j.biochi.2009.06.015.
[11] R. Shanmugakala, P. Tharmaraj, C.D. Sheela, N. Chidambaranathan, Transition metal complexes of s-triazine derivative: new class of anticonvulsant, anti-inflammatory, and neuroprotective agents, Med. Chem. Res. 23 (2014) 329–342, https://doi.org/10.1007/s00044-013-0634-0.
[12] B. Bhusan Subudhi, P.K. Panda, D. Bhatta, A. Jena, Anticonvulsant and antimicrobial activity of Cu (II), Zn (II) and Co (II) complex of Isatin 3-Glycine, Iran. J. Pharm. Sci. 5 (2009) 83–88.
[13] G.S. Kurdekar, M.P. Sathisha, S. Budagumpi, N.V. Kulkarni, V.K. Revankar, D. K. Suresh, 4-Aminoantipyrine-based Schiff-base transition metal complexes as potent anticonvulsant agents, Med. Chem. Res. 21 (2012) 2273–2279, https://doi.org/10.1007/s00044-011-9749-3.
[14] M.S. Hasan, N. Das, Z. Al Mahmud, S.M. Abdur Rahman, Pharmacological evaluation of naproxen metal complexes on antinociceptive, anxiolytic, CNS depressant, and hypoglycemic properties, Adv. Pharmacol. Pharm. Sci. 2016 (2016), e3040724, https://doi.org/10.1155/2016/3040724.
[15] N.V. Kulkarni, S. Budagumpi, G.S. Kurdekar, V.K. Revankar, S. Didagi, Anticonvulsant activity and toxicity evaluation of Cu^{II} and Zn^{II} metal complexes derived from triazole-quinoline ligands, Chem. Pharm. Bull. 58 (2010) 1569–1575, https://doi.org/10.1248/cpb.58.1569.
[16] A.T. Odularu, P.A. Ajibade, Dithiocarbamates: challenges, control, and approaches to excellent yield, characterization, and their biological applications, Bioinorg. Chem. Appl. 2019 (2019), e8260496, https://doi.org/10.1155/2019/8260496.
[17] C.I. Yeo, E.R.T. Tiekink, J. Chew, Insights into the antimicrobial potential of dithiocarbamate anions and metal-based species, Inorganics 9 (2021) 48, https://doi.org/10.3390/inorganics9060048.
[18] J.W. de F. Oliveira, H.A.O. Rocha, W.M.T.Q. de Medeiros, M.S. Silva, Application of dithiocarbamates as potential new antitrypanosomatids-drugs: approach chemistry, Funct. Biol. Mol. 24 (2019) 2806, https://doi.org/10.3390/molecules24152806.
[19] V. Bala, G. Gupta, V.L. Sharma, Chemical and medicinal versatility of dithiocarbamates: an overview, Mini Rev. Med. Chem. 14 (2014) 1021–1032.
[20] B. Cvek, Z. Dvorak, Targeting of nuclear factor-κB and proteasome by dithiocarbamate complexes with metals, Curr. Pharm. Des. 13 (2007) 3155–3167, https://doi.org/10.2174/138161207782110390.
[21] A. Rafiq, S. Aslam, N. ul A. Mohsin, M. Ahmad, Synthetic routes for the development of Piperazine-based acetanilides and their medicinal importance, Polycycl. Aromat. Compd. 0 (2023) 1–29, https://doi.org/10.1080/10406638.2023.2259561.
[22] D. Chen, Q.P. Dou, New uses for old copper-binding drugs: converting the pro-angiogenic copper to a specific cancer cell death inducer, Expert Opin. Ther. Targets 12 (2008) 739–748, https://doi.org/10.1517/14728222.12.6.739.
[23] W. Huang, Y. Ding, Y. Miao, M.Z. Liu, Y. Li, G.F. Yang, Synthesis and antitumor activity of novel dithiocarbamate substituted chromones, Eur. J. Med. Chem. 44 (2009) 3687–3696, https://doi.org/10.1016/j.ejmech.2009.04.004.
[24] T.N. Akhaja, J.P. Raval, New carbodithioate derivatives: synthesis, characterization, and in vitro antibacterial, antifungal, antitubercular, and antimalarial activity, Med. Chem. Res. 22 (2013) 4700–4707, https://doi.org/10.1007/s00044-013-0472-0.
[25] G. Hogarth, Metal-dithiocarbamate complexes: chemistry and biological activity, Mini Rev. Med. Chem. 12 (2012) 1202–1215, https://doi.org/10.2174/138955712802762095.

[26] P.A. Ajibade, A.A. Fatokun, F.P. Andrew, Synthesis, characterization and anti-cancer studies of Mn(II), Cu(II), Zn(II) and Pt(II) dithiocarbamate complexes - crystal structures of the Cu(II) and Pt(II) complexes, Inorg. Chim. Acta 504 (2020), 119431, https://doi.org/10.1016/j.ica.2020.119431.
[27] A. Singh, L.B. Prasad, K. Shiv, R. Kumar, S. Garai, Synthesis, characterization, and in vitro antibacterial and cytotoxic study of Co(II), Ni(II), Cu(II), and Zn(II) complexes of N-(4-methoxybenzyl) N-(phenylethyl) dithiocarbamate ligand, J. Mol. Struct. 1288 (2023), 135835, https://doi.org/10.1016/j.molstruc.2023.135835.
[28] S. Jaiswal, S.K. Pandey, J. Prajapati, S. Chandra, M.K. Gond, M.K. Bharty, I. Tiwari, R.J. Butcher, Cd(II) complexes derived from thiazoline, hydrazide and carbodithioate ligands: synthesis, crystal structures and electrochemical sensing of uric acid, Appl. Organomet. Chem. 37 (2023) e7085, https://doi.org/10.1002/aoc.7085.
[29] B. Arul Prakasam, M. Lahtinen, A. Peuronen, M. Muruganandham, E. Kolehmainen, E. Haapaniemi, M. Sillanpää, Spectral and structural studies on Ni(II) dithiocarbamates: nickel sulfide nanoparticles from a dithiocarbamate precursor, Inorg. Chim. Acta 425 (2015) 239–246, https://doi.org/10.1016/j.ica.2014.09.016.
[30] S.K. Pal, B. Singh, J.K. Yadav, C.L. Yadav, M.G.B. Drew, N. Singh, A. Indra, K. Kumar, Homoleptic Ni(II) dithiocarbamate complexes as pre-catalysts for the electrocatalytic oxygen evolution reaction, Dalton Trans. 51 (2022) 13003–13014, https://doi.org/10.1039/D2DT01971J.
[31] V. Singh, R. Chauhan, A.N. Gupta, V. Kumar, M.G.B. Drew, L. Bahadur, N. Singh, Photosensitizing activity of ferrocenyl bearing Ni(II) and Cu(II) dithiocarbamates in dye sensitized TiO2 solar cells, Dalton Trans. 43 (2014) 4752–4761, https://doi.org/10.1039/C3DT52142G.
[32] V. Milacic, D. Chen, L. Giovagnini, A. Diez, D. Fregona, Q.P. Dou, Pyrrolidine dithiocarbamate-zinc(II) and -copper(II) complexes induce apoptosis in tumor cells by inhibiting the proteasomal activity, Toxicol. Appl. Pharmacol. 231 (2008) 24–33, https://doi.org/10.1016/j.taap.2008.03.009.
[33] M. Shebl, O.M.I. Adly, H.F. El-Shafiy, S.M.E. Khalil, A. Taha, M.A.N. Mahdi, Structural variety of mono- and binuclear transition metal complexes of 3-[(2-hydroxy-benzylidene)-hydrazono]-1-(2-hydroxyphenyl)-butan-1-one: synthesis, spectral, thermal, molecular modeling, antimicrobial and antitumor studies, J. Mol. Struct. 1134 (2017) 649–660, https://doi.org/10.1016/j.molstruc.2017.01.012.
[34] Y.R. Zheng, Z.L. Chai, Y.F. Ding, L. Wang, W.K. Dong, Y.J. Ding, Exploring the effects of counterions and solvents on binuclear and tetranuclear Cu(II) oligo(N,O-donor) salamo-based complexes, J. Mol. Struct. 1295 (2024), 136729, https://doi.org/10.1016/j.molstruc.2023.136729.
[35] V.K. Maurya, L.B. Prasad, A. Singh, K. Shiv, A. Prasad, Synthesis, spectroscopic characterization, biological activity, and conducting properties of functionalized Ni(II) dithiocarbamate complexes with solvent extraction studies of the ligands, J. Sulfur Chem. 44 (2023) 336–353, https://doi.org/10.1080/17415993.2022.2157680.
[36] T.H. Ahern, M.A. Javors, D.A. Eagles, J. Martillotti, H.A. Mitchell, L.C. Liles, D. Weinshenker, The effects of chronic norepinephrine transporter inactivation on seizure susceptibility in mice, Neuropsychopharmacol 31 (2006) 730–738, https://doi.org/10.1038/sj.npp.1300847.
[37] B.D. Obay, E. Tasdemir, C. Tümer, H.M. Bilgin, A. Sermet, Antiepileptic effects of ghrelin on pentylenetetrazole-induced seizures in rats, Peptides 28 (2007) 1214–1219, https://doi.org/10.1016/j.peptides.2007.04.003.
[38] R.G. Lister, The use of a plus-maze to measure anxiety in the mouse, Psychopharmacology 92 (1987) 180–185, https://doi.org/10.1007/BF00177912.
[39] C. Belzung, G. Griebel, Measuring normal and pathological anxiety-like behaviour in mice: a review, Behav. Brain Res. 125 (2001) 141–149, https://doi.org/10.1016/S0166-4328(01)00291-1.
[40] J. Archer, Tests for emotionality in rats and mice: a review, Anim. Behav. 21 (1973) 205–235, https://doi.org/10.1016/S0003-3472(73)80065-X.
[41] R.P. Singh, A. Singh, L.B. Prasad, K. Shiv, S.K. Hira, P.P. Manna, Nickel (II), Copper (II), and Zinc (II) Complexes of N-bis (4-methoxybenzyl) dithiocarbamate: synthesis, characterization studies, and evaluation of antitumor activity, J. Mol. Struct. 1264 (2022), 133295, https://doi.org/10.1016/j.molstruc.2022.133295.
[42] L. Tong, L.L. Man, X. Li, W.K. Dong, Two novel quinoline-decorated half-salamo-type Co(II) complexes: synthesis, crystal structure, Hirshfeld surface analysis, DFT calculation and fluorescence properties, J. Mol. Struct. 1294 (2023), 136372, https://doi.org/10.1016/j.molstruc.2023.136372.
[43] Yuan-Ji Yan, Ya-Ting La, Ming-Xia Du, Li Xu, Wen-Kui Dong, Experimental and computational studies of two binuclear Co(II) and Ni(II) bis(salamo)-like complexes, Appl. Organom. Chem. (2023). https://onlinelibrary.wiley.com/doi/abs/10.1002/aoc.7214 (Accessed October 28, 2023).
[44] K.J. Colston, S.A. Dille, B. Mogesa, A.V. Astashkin, J.A. Brant, M. Zeller, P. Basu, Design, synthesis, and structure of copper dithione complexes: redox-dependent charge transfer, Eur. J. Inorg. Chem. 2019 (2019) 4939–4948, https://doi.org/10.1002/ejic.201901222.
[45] P. Nath, M.K. Bharty, B. Maiti, A. Bharti, R.J. Butcher, J.L. Wikaira, N.K. Singh, Ag (I), Cu(II), Co(III) and Hg(II) complexes and metal-assisted products derived from 4-methyl-piperidine-carbodithioate: syntheses, structures, thermal analyses, redox behaviour and fluorescence properties, RSC Adv. 6 (2016) 93867–93880, https://doi.org/10.1039/C6RA15186H.
[46] A. Bharti, P. Bharati, U.K. Chaudhari, A. Singh, S.K. Kushawaha, N.K. Singh, M. K. Bharty, Syntheses, crystal structures and photoluminescent properties of new homoleptic and heteroleptic zinc(II) dithiocarbamato complexes, Polyhedron 85 (2015) 712–719, https://doi.org/10.1016/j.poly.2014.10.002.
[47] Structural diversity in the mercury(II) bis(N,N-dialkyldithiocarbamate) compounds: an example of the importance of considering crystal structure when rationalising molecular structure, Z. Kristallogr. - Cryst. Mater. 214 (1999) 571–579, https://doi.org/10.1524/zkri.1999.214.9.571.
[48] I.P. Ferreira, G.M. De Lima, E.B. Paniago, C.B. Pinheiro, J.L. Wardell, S.M.S. V. Wardell, Study of metal dithiocarbamate complexes, Part V. Metal complexes of [S2CN(CH2CH(OMe)2]: a standard dimeric zinc dithiocarbamate structural motive, a rare cadmium dithiocarbamate coordination polymer, and a hydrated sodium dithiocarbarmate complex, with a[Na2O2] core and chain, Inorg. Chim Acta 441 (2016) 137–145, https://doi.org/10.1016/j.ica.2015.11.011.